IJHSR ijhighschoolresearch.org

RESEARCH ARTICLE

Using a Deep Neural Network to Downscale a General Circulation Model at the National Scale in Australia

Alex H. Zhuang

The King's School, 87-129 Pennant Hills Road, North Parramatta, NSW, 2159, Australia; zhuanghuijie2008@gmail.com
Mentor: Joe Xiao

ABSTRACT: General Circulation Models (GCMs) are powerful tools for simulating future climate change, but have suffered from low-resolution outputs that are unusable for local and regional planning and budgetary bodies. This study aims to downscale GCM-simulated annual rainfall data at the national scale in Australia, representing the largest-scale GCM downscaling study in Australian Literature. This study collected over 69000 data points containing hydrological variables and mapped them within GIS software. These data points were arranged in a grid with a spacing of 10km between points, an effective 100-fold increase in detail from the original GCM resolution of 10000 km^2. The data were used to train a Deep Neural Network, which achieved an average prediction accuracy of ±7% from the observed rainfall value, with an R-squared value of 0.991. Analysis of the neural network suggests the significant importance of rainfall and humidity to model predictions, indicating that local relative rainfall distribution depends on rainfall and humidity rather than temperature. With this model, we enable local governmental and budgetary bodies to make informed decisions in response to future climate change impacts, such as for State Emergency services and Infrastructure development efforts.

KEYWORDS: Earth and Environmental Science, Water Science, Neural Network, Downscaling, Climate Model, GCM Downscaling.

Introduction

Australia is known for its natural wonders, but the same environment has been causing increasing damage due to climate change. According to the Insurance Council of Australia Insurance Catastrophe Resilience Report 2025, damages from climate-related extreme-weather events are projected to increase to $35.2 billion in Australia by 2050, with climate change further increasing rainfall intensity and flood frequency in Australia's densely populated coastline. To reduce or prevent these potential damages, local and regional budgetary and planning bodies need access to useful data on future climate projections to make effective, informed decisions. Accurate future projections both allow first responders (State Emergency Services, Fire Service, Ambulance, Police) more time to prepare and provide present local governmental bodies with incentives to make sustainable decisions.[1-3]

Climate models, specifically General Circulation Models (GCMs), have provided key insights into the potential global impacts of climate change scenarios, but they lack the high-resolution, local-scale detail of traditional weather forecasts for use by local government bodies.[4] It is important to recognize the distinction between climate models and traditional weather forecasts: GCMs are primarily used to simulate future rainfall under defined atmospheric conditions,[4] whereas weather forecasts predict near-future rainfall using concurrent observations of local climate.[5] GCMs operate by physically simulating atmospheric circulation within a defined column of air above the ground, thereby requiring large simulation cells to capture complex large-scale atmospheric processes, but at the expense of output detail.[4] To gauge climate change impacts, climate model developers input a hypothetical climate scenario, for example, the atmosphere with 600 ppm carbon dioxide, into the GCM and analyze the output. For use in local and regional impact assessment, GCM output needs to be appropriately downscaled to a higher resolution.[4]

GCM downscaling is separated into two main methodologies: dynamical and statistical downscaling.[6] Dynamical downscaling involves operating a climate model at a higher spatial resolution, producing output with higher spatial resolution.[6] This can be done at a global scale or, more commonly, in Regional Climate Models (RCMs), which generate climate simulations within a defined area of the Earth. The downsides are that dynamical downscaling requires physical access to the climate model's code and programs to produce higher-resolution results, which is highly computationally intensive.[2, 6] It also relies on the creators of the GCM to manually produce downscaled results or to create a corresponding RCM, which means that GCM-derived RCMs for specific regions of the world, for example, the Australian state of New South Wales, are not available.[3] Additionally, as this study did not develop or have the source code for a GCM, this study did not utilize the dynamical approach. Conversely, Statistical downscaling uses observed relationships between climate model outputs and local atmospheric conditions to train a separate model.[6] Unlike dynamically downscaled models, statistical models utilize the GCM output only as an input variable, among other climatological variables, with a provided ground truth to compare the predicted rainfall of the model with actual rainfall.[7, 8] As such, statistical downscaling models do not require physical access to the GCM's operating code to make predictions, only its output

DOI: 10.36838/IJHSR817.1

data, other gathered inputs, and observed variables.[6] However, traditional methods of statistical downscaling generally require large, diverse datasets derived from complete atmospheric measurements from select weather stations,[9] which are not available at a national scale. Moreover, they are often complicated models,[7,8] requiring detailed, long-term observation of the ground truth for the model to construct a statistical relationship between the predictors and the observed values.[6] As a result, traditional statistical downscaling models have the drawback of an overly narrow focus on local and catchment scales.[1,9-11]

The method employed in this study (regressing rainfall using a deep learning neural network) is a statistical downscaling approach. This study seeks to build on existing literature by downscaling GCM outputs at the national scale, an area of orders of magnitude larger than those in previous Australian Literature, which often focuses on downscaling within a specific catchment basin.[1,9-11] Research conducted in Australia, such as Timbal *et al.*, downscales GCM data within specific "areas of interest", specifically being the Murray-Darling Basin, Nullarbor Plain, South East Coast, Tasmania, South East Australia, and South West Australia regions.[1] This reflects the aforementioned tendency for Australian climate downscaling studies to downscale within state and catchment-sized scales, not at the national scale. Internationally, studies such as Ahmed *et al.* and Polasky *et al.* downscale climate data at the state scale,[9,11] with the former downscaling precipitation in the Balochistan region of Pakistan and the latter downscaling GCMs in the Midwest United States. To bridge this gap in national-scale GCM downscaling, a machine learning approach was used to achieve acceptable regression accuracy whilst simultaneously requiring less computational power and reducing the complexity of the required dataset. Previous studies that utilize a machine-learning downscaling approach include Ahmed *et al.* and Wilby *et al.* These studies gather large amounts of atmospheric and GCM data, as well as ground-truth data from measured, time-series climate data in the real world corresponding to the GCM variable.[9,12] This study's methodology is based on the methodologies established in the two ML-based papers above, outlined in Figure 1 with a flowchart.

Methods

Study area:

The study area covers the entire extent of continental Australia, including Tasmania. Australia features a predominantly arid interior, with temperate climates in the East.[13] The Great Dividing Range in Australia's east blocks rainfall from the sea from reaching the desertified interior, causing Australia's east to experience temperate to tropical conditions with significant rainfall variability. In the states of Queensland and the Northern Territory, temperate grasslands gradually transition to tropical rainforest conditions, creating pockets of extremely high average annual rainfall.[13]

Data sources

The data used in this study were obtained from multiple sources. Decadal-averaged data and ground-truth annual observed rainfall were obtained from the Australian Bureau of Meteorology climate maps.[14] The observed rainfall is available only at the monthly scale, so the extracted monthly values must be aggregated to obtain the 2024 yearly observed rainfall. To source elevation data, the GEODATA 9-second Digital Elevation Model 2008 3.0 was downloaded from Geoscience Australia,[15] covering all of Australia. The climate model output used originated from the Italian CMCC-CM2-SR5 General Circulation Model,[16] and was obtained via the European Network of Earth System Modeling (ENES) Climate4Impact portal.[17] Specifically for this climate model, hindcast data for 2024 were used, which correspond to the observed 2024 rainfall data from the Australian Bureau of Meteorology, which served as the ground truth for the model.

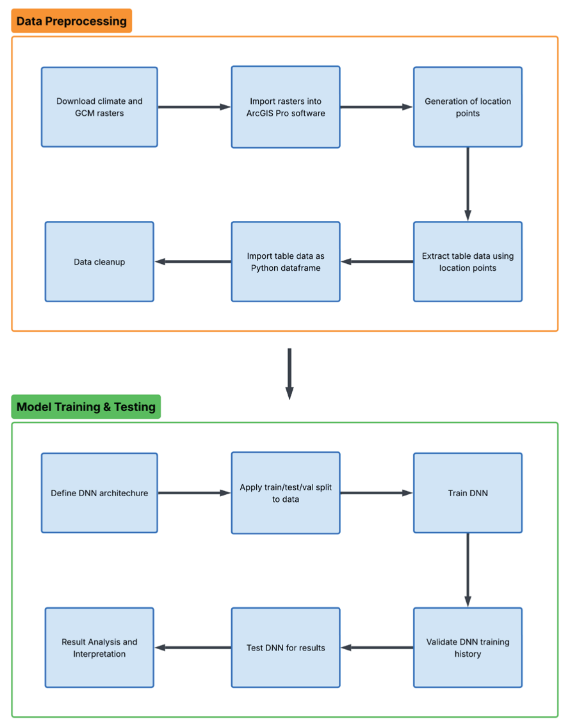

Figure 1: Methodology flowchart of this study. The methodology is split into two main stages in chronological order: the data collection and model training stages, respectively.

Data preprocessing:

The dataset was split into two components: predictors and labels. The predictors include spatially variable data or otherwise simulated data that lack a direct temporal reference. This includes historical averages of rainfall and humidity, derived from measurements over the past decades, and is assumed to be indicative of future observed values. Note that the GCM hindcast 2024 output is a predictor, as the GCM output is not dependent on observations made in the year 2024, but instead simulated using 2024's expected atmospheric composition. Therefore, the GCM can generate outputs for future years and serve as a predictor. Other climatological variables were selected based on prior research, namely observed annual rainfall, annual average humidity (measured at 9 am and 3 pm), elevation, and annual temperature (maximum, minimum, and mean).1 As the model aims to replicate the long-term rainfall distribution within a large-scale GCM cell, an adjustment was made to use the spatially variable versions of these otherwise short observational time series. The rainfall, humidity, and temperature used are 30-year climatological averages across Australia. These values are assumed to be effectively constant when downscaling GCM outputs of near-future climate conditions. The label group comprises exclusively observed rainfall data, specified by the GCM hindcast date. As seen in Table 1 below, 8 input variables and 1 observed variable, against which the model output is compared, are used.

Table 1: Table of input variables used in the model with associated meaning and units. The 30-year climatology in this table is the same for all associated variables, being averages of the yearly values over the period 1990-2020.

Variable name	Meaning	Units
GCM_Hindcast_2024	Simulated rainfall value within a GCM cell, output as an average over a set year at a location	Millimeters (yearly total)
average_annual_rainfall	Total rainfall value averaged over a 30-year climatology (1990-2020) at a location	Millimeters (yearly total)
9am_humidity	Average 9 am humidity taken at a location over a 30-year climatology	% Relative humidity
3pm_humidity	Average 9 am humidity taken at a location over a 30-year climatology	% Relative humidity
elevation	Elevation above sea level at a location	Metres
mean_annual_temperature	The average of the mean yearly observed temperatures over a 30-year climatology	Degrees Celsius
min_annual_temperature	The average of the minimum yearly observed temperatures over a 30-year climatology	Degrees Celsius
max_annual_temperature	The average of the maximum yearly observed temperatures over a 30-year climatology	Degrees Celsius
2024_Yearly_Observed	Total observed rainfall at a location in the Year 2024.	Millimeters (yearly total)

Each variable defined in Table 1 was originally available as a raster or a geographical heatmap. A raster map is composed of individual pixels of a specified geographical size resolution, and is combined to form a large map image of the specified raster area. Each pixel, also known as a raster cell, holds a specific value and is often visualized in Geographic Information Systems (GIS) software using a color gradient that denotes the relative magnitude of the value in the cell. As seen in Figure 2, these rasters can spatially overlap, necessitating their distinction using different color gradients.

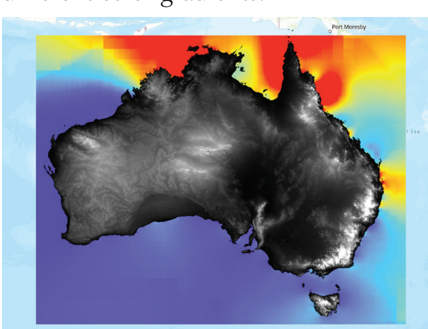

Figure 2: The elevation raster (black & white) overlaying the observed rainfall January 2024 raster (Colored). The color gradient in each raster (white to black and red to blue, respectively) indicates the relative magnitude of feature values in a raster cell. The rainfall raster lies beneath the elevation raster by virtue of the draw order in GIS software, demonstrating how the rasters used geographically overlap on the Australian Landmass.

Data preprocessing - Generation of datapoints:

Data in this study encompass a rectangular area with top-left and bottom-right bounds of 112.74°E, 10.27°S, and 156.04°E, 43.87°S, respectively. Because raw climatological data are typically available in raster form, they must undergo extensive preprocessing before they can be used in the neural network. The raster datasets were first loaded into ArcGIS Pro,[18] resulting in multiple geographically overlapping raster datasets, as all rasters have defined data within Australia.

To convert this data into a table, coordinate points were generated in ArcGIS Pro for use with the Extract Multi Values to Points tool.[18] The Extract Multi Values to Points tool in ArcGIS Pro operates by identifying the raster cell that spatially coincides with each input point and retrieving the cell value at that location.[18] It performs this process for all selected raster layers (e.g., rainfall observed, GCM raster, humidity average). The result is a feature matrix in which each row corresponds to a point, and each column contains the extracted values from the corresponding raster datasets. As shown in Figure 3, the aforementioned coordinate points are individual locations. The exported feature matrix is ultimately used as the model's input, with each row corresponding to a location point and therefore a data sample.

Figure 3: Simplified version of datapoints drawn in ArcGIS Pro.[18] The actual data points used are far more numerous and distributed across a far denser grid than shown in the image, which occupies each humidity raster cell.

To downscale the GCM raster correctly, the point grid must be configured so that multiple points fall within each large GCM cell, while each point lies in a different cell for the higher-resolution predictor rasters. This ensures that only the climate model output is being spatially downscaled, while the other environmental variables contribute unique, location-specific information to generate valid predictions. To achieve this, the point density was set to the cell size of the lowest-resolution predictor raster beside the GCM raster - the humidity raster with a resolution of 0.1° × 0.1° (approximately 10 km × 10 km). Using this spacing, 146,258 coordinate points were generated, forming a continuous point grid across the entire contiguous Australian mainland and Tasmania.

Figure 4 below illustrates the concentration of data points by overlaying the data point grid on the GCM and humidity rasters in a given region. Specifically, the figure overlays the Australian coastal city of Port Macquarie, which was arbitrarily chosen for this example. As seen in Figure 4(a), 96 data points are located within the central GCM raster cell depict-

DOI: 10.36838/IJHSR817.1

ed in yellow, which downscales the GCM raster and predicts rainfall values for each data point. As seen in Figure 4(b), each humidity raster cell contains only one data point, providing the model with a spatially unique humidity value for a valid prediction. Thus, Figure 4(b) shows the maximum spatial density of data points possible for this study, which was ultimately used for data extraction. It is important to note that a less spatially dense data point grid can be used for data extraction. A valid prediction does not require that each humidity raster cell be used for all input data, just that the data points must each represent spatially unique data, where no two data points can occupy the same cell of any non-GCM rasters. In higher-resolution rainfall rasters, for example, the temperature raster, the data points occupied only one in four cells on average.

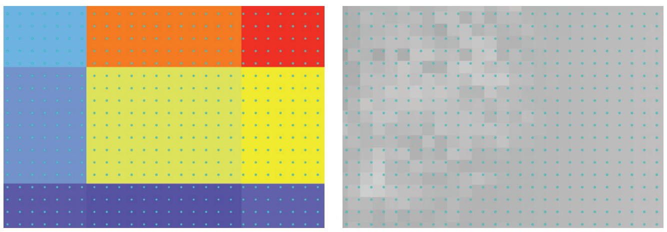

(a) GCM Raster. The central grid cell size is 100 km by 100 km. Surrounding cells are cropped. The color gradient from red to blue represents high to low-value cell attribute values, respectively. Blue dots are data points spaced 10 km by 10 km.

(b) Humidity Raster. Cell size is 10 km by 10 km. Edge cells are cropped. The color gradient from white to black represents high to low cell attribute values, respectively. Blue dots are data points spaced 10km by 10km.

Figure 4: Generated data points (blue) overlaying the GCM Raster (a) and the Humidity raster (b). Around 100 data points are contained within each GCM raster cell, while a humidity raster cell only contains 1 data point. The area is an aerial shot of Port Macquarie, New South Wales, Australia.

Because some original data point locations contained many values over the ocean, the data needed to be filtered to eliminate data points that lacked complete data across all selected rasters. This is because the individual rasters have different sizes: the GCM raster is global-scale, the elevation raster covers only Australian land, and others cover land and the nearshore ocean. The simplest way to filter is to delete all data from datapoints without a specified elevation value, as the elevation raster is the smallest and is included within all other raster maps, meaning that a datapoint geographically overlapping the elevation raster must therefore be included in all other raster maps as well. This leaves 69581 usable datapoints, from the original 146258, for training and testing the model.

All monthly observed rainfall totals were summed to obtain the 2024_Yearly_Observed value, which was used as the label. The GCM_Hindcast_2024 raster data was averaged over a year to mm/s, then multiplied by 31556926 (the number of seconds in a year) to extrapolate the yearly GCM value for 2024, ensuring all rainfall variables were in units of mm/year.

Deep Neural Network (DNN) Model:

A deep neural network was used in this study, based on prior findings that neural networks consistently yielded lower Root Mean Squared Error (RMSE) values than traditional statistical downscaling methods, which instead used first-order two-state Markov processes, binomial occurrences, and vorticity-based resampling.[12] Although DNNs noticeably suffer when attempting to predict the random occurrence of rainy days,[12] this study does not face this limitation. As this study performs downscaling at the annual time scale, each prediction represents the sum of many daily rainfall values. When many daily observations are aggregated, the resulting annual total tends to exhibit a more symmetric and stable distribution. Under the Central Limit Theorem, the sum of a large number of daily rainfall amounts with finite variance will approximate a normal distribution, reducing sensitivity to inaccuracies in simulating individual extreme wet days.

Model Architecture:

The DNN has 8 input neurons, 6 hidden layers with 30 neurons each, and 1 output neuron. This specific combination of parameters was selected through a manual search in hyperparameter tuning, which aims to identify the best-performing model architecture. This model is a Deep Neural Network (DNN) because it has more than one hidden layer. The Rectified Linear Unit (ReLU) activation function was applied between layers, constraining values to either zero or positive.

The 8 input neurons and 1 output neuron are defined by the number of selected input variables and the required regression outputs, which are fixed and cannot be changed. Therefore, tests to find the optimal model architecture were conducted using a grid search to determine the number of hidden layers and the number of neurons per hidden layer. All tested model parameters are shown below, in increments of 1 for hidden layers and 10 hidden neurons for a total of 25 manual tests.

Tested number of hidden layers: [3, 4, 5, 6, 7}

Tested hidden neurons per hidden layer: [10, 20, 30, 40, 50]

DNN Training Loop:

The training loop is configured to take a data batch size of 10, and Mean Squared Error (MSE) loss was used in the model. This process includes computing the error as a function of the model weights, then finding the gradient as the partial derivative of the loss with respect to the model weights. The model weights are then updated in the opposite direction, reducing the error in a process known as gradient descent. In this study, the Adam optimizer was used.[19]

The overall dataset was randomly split into training (64%, 44531 samples), validation (16%, 11133 samples), and test (20%, 13917 samples) sets. The model was set to train for 1500 epochs. To ensure model convergence and prevent overfitting, early stopping was implemented with a patience of 100 epochs.

Results and Discussion

The model with 6 Layers and 30 hidden neurons per layer achieved the lowest Root Mean Square Error (RMSE), while simpler networks failed to capture and predict rainfall values with acceptable accuracy. Models with more hidden layers and more hidden neurons achieved similar accuracy but required significantly longer training times and were therefore deemed suboptimal.

The model converged after 1338 epochs of training, with the MSE reduction following an exponential decay pattern, as shown in Figure 5. The neural network's predictions on the test set had an RMSE of around 40mm/year, with the average label value being around 600mm/year. This represents an effective error of ±7% relative to the predicted value, which is within the acceptable ±25% accuracy threshold for short-term rainfall forecasts.[5]

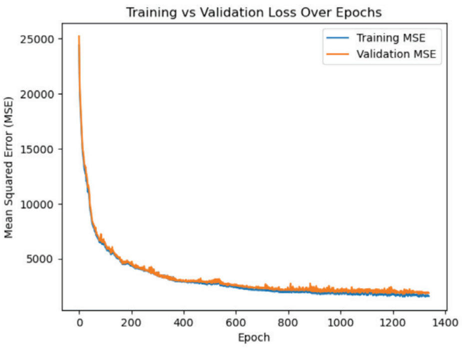

Figure 5: Model error across epochs of training. MSE on the training and validation sets was graphed separately to inspect the model for overfitting, which would cause Validation MSE to be significantly higher than Training MSE. The close alignment of training and validation MSE curves demonstrates that the model has not overfitted to the training data.

An R-squared value indicates the percentage of variance in the predicted values explained by the variance among the predictor variables. In simple terms, it is the percentage variation in the final value that can be explained by the predictors. A high R-squared value of 0.9-1 indicates that the predictors account for the majority of the variation in the output variables, indicating a statistically valid prediction. R-squared alone, however, does not reveal the full extent of a model's accuracy, as systematic biases towards certain predictor variables or value ranges can reduce the model's prediction quality while maintaining a high R-squared value. Therefore, this study uses additional methods, such as RMSE, predicted vs. actual, and residual vs. actual graphs, as well as SHAP analyses, to fully assess the model's accuracy across all predicted and error ranges. The results of those tests are outlined further below.

The R-squared value calculated between the observed and predicted values of the model averaged around 0.991, meaning that 99.1% of the variance in the observed values can be explained by the variance in the predicted values. This suggests that the model and its input variables account for the vast majority of factors contributing to the final yearly total rainfall, reinforcing the ±7% accuracy previously found with RMSE. R-squared values this high may suggest data leakage between the predictor variables and the target label, undermining the validity of the model's predictions. In this case, the main concern is potential leakage between the GCM hindcast rainfall predictor and the observed ground-truth rainfall used as the label. This is because observed rainfall totals are incorporated into the GCM hindcast dataset to bias-correct the model output toward real observations when generating the hindcast rasters of the CMCC-CM2-SR5 General Circulation Model.[16] However, this hindcast data is generated at the decadal scale,[16] averaged over the years 2014-2024. The data used to validate the climate model hindcast must therefore have been captured in 2014, which validates the R-squared value, as the possibility of the GCM bias-correcting to the 2024 annual observed rainfall value was ruled out. Furthermore, the GCM data was installed before the migration of the European Network for Earth Systems Modeling (ENES) server infrastructure in December 2024, ruling out data leakage, as the Australia-wide annual rainfall total data for 2024 did not yet exist.

As seen in Figure 6 below, the model predictions closely align with the theoretical perfect accuracy, with RMSE = 0, as denoted by the line y = x across the entire range of predicted and actual values. Although most values cluster in the 0-2000 mm rainfall per year range in Figure 6, the extremes in the 3000-5000 mm range also align closely with the line, suggesting that the model provides accurate predictions for both low and extremely high rainfall in Australia. This also suggests that the earlier RMSE value is not distorted by any significant outliers, and that an error within ±7% of the observed value is an effective measure of model accuracy.

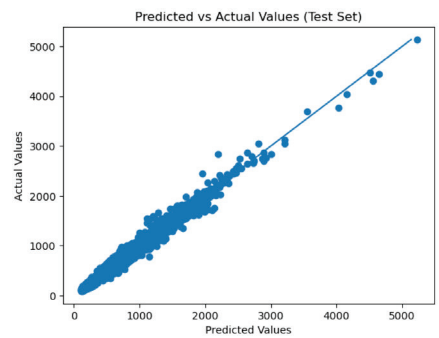

Figure 6: Predicted vs Actual values graph. The predicted vs actual values graph is used to gauge model performance across a wide range of values. Each dot in the graph represents a single prediction from the model on the test split of the dataset. This graph pattern indicates that the model has low error across the entire range of predicted rainfall values.

As illustrated in Figure 7, the distribution of residuals against actual values shows no discernible patterns or systematic biases. This uniform performance validates the high R-squared and RMSE values, ensuring they are not skewed by specific data ranges. The clustering of the dots in the 0 - 2000 mm range on the left side of Figure 7 indicates only the frequency of data points with actual values in that range and does not indicate any systematic error.

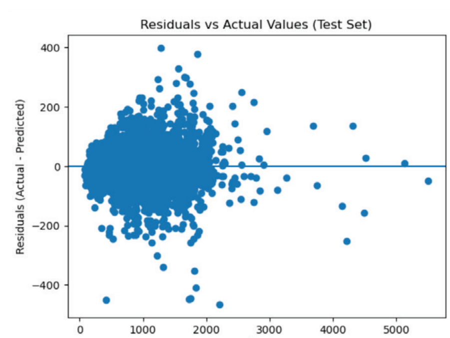

Figure 7: Residuals vs actual scatter plot. Each dot is a model prediction on the test set, with the 0 line indicating a perfect prediction. Dots above and below the line represent overpredictions and underpredictions, respectively. Randomly scattered dots above indicate that the model is not systematically biased towards any range.

DOI: 10.36838/IJHSR817.1

A SHAP analysis was used to quantify the individual contributions of selected variables to the neural network's output.[20] As seen in Figure 8, the variable with the greatest contribution is the decadal average annual rainfall variable, due to its greatest range of SHAP values, followed by the GCM output, and then closely by the two humidity variables. This analysis suggests that the model is utilizing predominantly rainfall and humidity values for prediction, indicating that local relative rainfall distribution is determined predominantly by rainfall and humidity variations rather than temperature.

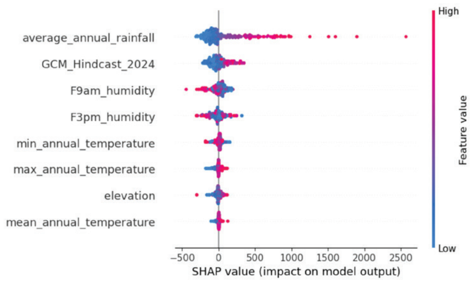

Figure 8: SHAP analysis of the neural network. The 8 input variables are listed on the left, with their contributions shown on the bottom as a scale. Each point in the middle is an instance of the corresponding input variable, with the point's SHAP value coming from a single prediction of the test set. This allows us to interpret the DNN and gauge which climate phenomena contribute to annual rainfall the most.

Limitations and considerations:

The model, by making a prediction, effectively simulates rainfall distribution within a specified General Circulation Model Cell at a 10 km by 10 km resolution. This study does not use time-series data as predictors. The model views the modeled rainfall distribution as a static factor that dictates predictions. This distribution was modeled based on the 30-year average annual climatology for 1990-2020, meaning the predictions could be reasonably extrapolated into the near future. An obvious limitation to this approach is that climate conditions are not static. This means that future changes in climate composition and atmospheric processes due to climate change cannot be accurately modeled using the 30-year climatological average data used in this study. Therefore, the model needs to be periodically retrained using new decadal-average rainfall data.

This model also assumes that the relative rainfall distribution within the spatial extent of a GCM cell will remain constant across different climate conditions. This assumption was made because climate change alters predominantly mean precipitation levels across a wide region rather than the relative distribution or concentration of precipitation within a select area,[21] suggesting that regional relative rainfall distribution is a product of temporally static, likely topological factors. Without this assumption of a static, localized, relative rainfall distribution, the model would need to physically simulate rainfall and precipitation processes in a 100 km by 100 km area for each data point, which is not within the scope of this study, as it would effectively make the model a dynamically downscaled GCM.

To explain this assumption, imagine an arbitrary GCM grid cell that overlaps City A and City B, with City A receiving twice the amount of rainfall as City B. In a hypothetical climate scenario, this study assumes the relative rainfall distribution within a GCM cell is constant, meaning that City A still receives twice the rainfall as City B despite drastic changes in the area-average rainfall. While near-future local rainfall distribution could be modeled statically under this assumption, changes to anthropogenic land use, significant changes to regional topography, and significant changes to climate conditions could alter this rainfall distribution, rendering model predictions for the far future or under extreme climate conditions invalid with high error.

Future directions:

While this study effectively predicts annual rainfall at a specified location, it does not estimate the frequency or temporal distribution of rainfall within a specific year. Future research could use the initially separate monthly ground-truth values to predict rainfall at the monthly temporal scale, or use daily total data from the Australian Bureau of Meteorology to predict rainfall at the daily temporal scale. Alternatively, future research could independently model the temporal distribution of rainfall over a year, using the data generated by this study's model as an input variable. Physical climate simulations could also be used in the aforementioned research, given the El Niño Southern Oscillation's significant impact on Australian precipitation distribution,[13] among other factors not included in this study, such as wind speed, air pressure at set altitudes, and surface divergence.[9, 22]

Future research could also aim to increase the resolution of the downscaled data by using a higher density of data points than in this study. This study was limited by the coarse resolution of the 9 am and 3 pm humidity datasets, which necessitated downsampling to 10 km by 10 km. Although useful for regional and local-scale applications, this data could be considered too coarse for extremely narrow use cases, such as suburb-scale planning and budgetary concerns. As such, research utilizing a finer-resolution humidity raster at the national scale can significantly increase detail, further expanding the study's possible applications. A possible barrier is that high-resolution climatological raster datasets are rare at the national scale, which could be addressed by splicing multiple high-resolution local rasters into a national raster for a specified variable. For specialized regional applications of GCMs that require higher resolution, this machine learning approach could be used in conjunction with dynamically downscaled RCM rasters for a defined region to achieve even higher-resolution and more accurate predictions. As dynamically downscaled RCMs typically have a resolution of 1 - 2 km per grid cell, a further statistical downscaling model could result in predictor data point separation of 100 - 200 m, a 10-fold increase in downscaled resolution from this study.

Conclusion

In this study, we downscaled the output of the CMCC-CM2-SR5 General Circulation Model at a national scale in Australia, the largest scale of climate model downscaling achieved in Australian literature. The DNN model used in this research predicts rainfall with an average prediction accuracy of ±7% relative to the mean and an R-squared value of 0.991, well within the acceptable error bound of ±25% for weather forecasting. The SHAP analysis suggests a greater contribution of the GCM, rainfall, and humidity variables than of temperature, indicating that local relative rainfall distribution is determined predominantly by rainfall and humidity variations rather than temperature. The downscaled resolution of 10 km by 10 km, effectively a 100x increase in detail from the original climate model output, allows local councils and budgetary bodies to make informed decisions in response to future climate change. Through this study, we lay a stepping stone in the nationwide availability of GCM model results, which we hope will allow future researchers to explore this critical field further.

Acknowledgments

This study would like to thank the Currie Country Social Change organization for their continued support of our research, informing our previous studies as well as similar flood research studies to the Australian Parliament regarding flood impacts on Indigenous Australians.

References

1. Timbal, B., Fernandez, E., & Li, Z. (2009). Generalization of a statistical downscaling model to provide local climate change projections for Australia. *Environmental Modeling & Software, 24*(3), 341–358. https://doi.org/10.1016/j.envsoft.2008.07.007
2. Xu, Z., Han, Y., & Yang, Z.-L. (2018). Dynamical downscaling of regional climate: A review of methods and limitations. *Science China Earth Sciences, 62*. https://doi.org/10.1007/s11430-018-9261-5
3. L.pez-G.mez, I., Wan, Z. Y., Zepeda-N. ez, L., Schneider, T., Anderson, J., & Sha, F. (2024). *Dynamical-generative downscaling of climate model ensembles* (arXiv:2410.01776). arXiv. https://doi.org/10.48550/arXiv.2410.01776
4. Intergovernmental Panel On Climate Change (IPCC). (2023). *Climate Change 2021 – The Physical Science Basis: Working Group I Contribution to the Sixth Assessment Report of the Intergovernmental Panel on Climate Change* (1st ed.). Cambridge University Press. https://doi.org/10.1017/9781009157896
5. Shahrban, M., Walker, J. P., Wang, Q. J., Seed, A., & Steinle, P. (2016). An evaluation of numerical weather prediction-based rainfall forecasts. *Hydrological Sciences Journal, 61*(15), 2704–2717. https://doi.org/10.1080/02626667.2016.1170131
6. Tang, J., Niu, X., Wang, S., Gao, H., Wang, X., & Wu, J. (2016). Statistical downscaling and dynamical downscaling of regional climate in China: Present climate evaluations and future climate projections. *Journal of Geophysical Research: Atmospheres, 121*(5), 2110–2129. https://doi.org/10.1002/2015JD023977
7. Sachindra, D. A., Huang, F., Barton, A., & Perera, B. J. C. (2014a). Statistical downscaling of general circulation model outputs to precipitation—part 1: Calibration and validation. *International Journal of Climatology, 34*(11), 3264–3281. https://doi.org/10.1002/joc.3914
8. Sachindra, D. A., Huang, F., Barton, A., & Perera, B. J. C. (2014b). Statistical downscaling of general circulation model outputs to precipitation—part 2: Bias-correction and future projections. *International Journal of Climatology, 34*(11), 3282–3303. https://doi.org/10.1002/joc.3915
9. Ahmed, K., Shahid, S., Harun, S., & Wang, X. (2015). Multilayer perceptron neural network for downscaling rainfall in arid region: A case study of Baluchistan, Pakistan. *Journal of Earth System Science, 124*, pp. 1325- 1341. https://doi.org/10.1007/s12040-015-0602-9
10. Liang, X.-Z., Kunkel, K. E., Meehl, G. A., Jones, R. G., & Wang, J. X. L. (2008). Regional climate models downscaling analysis of general circulation models presents climate biases propagation into future change projections. *Geophysical Research Letters, 35*(8). https://doi.org/10.1029/2007GL032849
11. Polasky, A. D., Evans, J. L., Fuentes, J. D., & Hamilton, H. L. (2022). Statistical climate model downscaling for impact projections in the Midwest United States. *International Journal of Climatology, 42*(5), 3038–3055. https://doi.org/10.1002/joc.7406
12. Wilby, R. L., Wigley, T. M. L., Conway, D., Jones, P. D., Hewitson, B. C., Main, J., & Wilks, D. S. (1998). Statistical downscaling of general circulation model output: A comparison of methods. *Water Resources Research, 34*(11), 2995–3008. https://doi.org/10.1029/98WR02577
13. Raktima, D., Lewis, S. C., Alblaster, J. M., Abram, N. J. (2019). A review of past and projected changes in Australia's rainfall. *Wires Climate Change*. https://doi.org/10.1002/wcc.577
14. Australian Government Bureau of Meteorology. Climate. https://www.bom.gov.au/climate/ (accessed 13 June 2024)
15. Australian Government Geoscience Australia. Digital Elevation Data. https://www.ga.gov.au/scientific-topics/national-location-information/digital-elevation-data (accessed 23 March, 2025)
16. Nicolì, D., Bellucci, A., Ruggieri, P., Athanasiadis, P., Materia, S., Peano, D., Fedele, G., & Gualdi, S. (2022). *The CMCC Decadal Prediction System*. Climate and Earth system modeling. https://doi.org/10.5194/gmd-2022-181
17. IS-ENES. Climate4Impact. https://www.climate4impact.eu/c4i-frontend (Accessed November 19, 2024)
18. Esri. ArcGIS Pro, version 2025 3.0.1; Environmental Systems Research Institute: Redlands, CA, 2025.
19. Kingma, D. P., & Lei, J. (2015). *Adam: A Method for Stochastic Optimization.*
20. Lundberg, S., & Lee, S.-I. (2017). *A Unified Approach to Interpreting Model Predictions* (arXiv:1705.07874). arXiv. https://doi.org/10.48550/arXiv.1705.07874
21. Nazeri Tahroudi, M. (2025). Comprehensive global assessment of precipitation trend and pattern variability considering their distribution dynamics. *Scientific Reports, 15*(1), 22458. https://doi.org/10.1038/s41598-025-06050-5
22. Rampal, N., Gibson, P. B., Sood, A., Stuart, S., Fauchereau, N. C., Brandolino, C., Noll, B., & Meyers, T. (2022). High-resolution downscaling with interpretable deep learning: Rainfall extremes over New Zealand. *Weather and Climate Extremes, 38*, 100525. https://doi.org/10.1016/j.wace.2022.100525

Author

Alex Huijie Zhuang studies at The King's School, Parramatta. Alex is a former member of the Australian National Earth Science Olympiad Team, winning a Gold individual medal at the 2025 International Earth Science Olympiad. His research in flood prediction was recognized at ISEF 2024 with a Third Place Award. Contact at zhuanghuijie2008@gmail.com

DOI: 10.36838/IJHSR817.1